

An Illustrated and Illustrative Tour of Recent Work with CP2K

Ben Slater

b.slater@ucl.ac.uk



Elias Garcia Martinez (1930)



Elias Garcia Martinez (1930)





Elias Garcia Martinez (1930)



Elias Garcia Martinez (1930)



FX Coudert @fxcoudert · Jan 6

"Our simulation method gives good qualitative agreement"

#ESRenPeinture



32



56



**Selected examples of work on
porous materials and ice**

Zeolites: Hybrid Functionals/ADMM

Ice: SS-NEB

MOFs: REPEAT scheme

SCAN functional

Ice: RPA/MP2

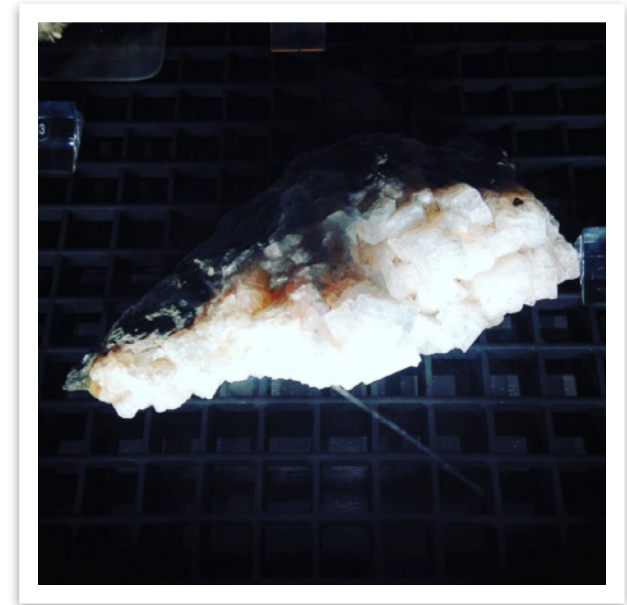
Elucidating framework aluminium distribution in catalytic zeolites



Rachel Fletcher Dr. Sanliang Ling

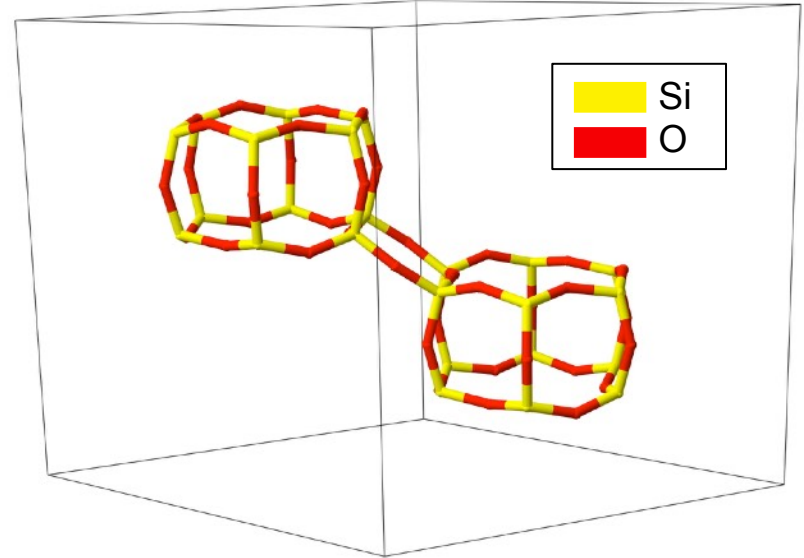
*R.E. Fletcher, S. Ling, B. Slater, 'Violations of Löwenstein's rule in zeolites' (2016)
arXiv:1612.04162 [cond-mat.mtrl-sci]*

- Microporous, crystalline aluminosilicate solids
- Petrochemical processing
 - Cracking, isomerisation and alkylation
- Increasing concern for the environment has motivated development of sustainable and environmentally benign alternatives to traditional petrochemical methods
- The use of traditional zeolite catalysts in atypical processes
 - Pollution control
 - Hydrocarbon production



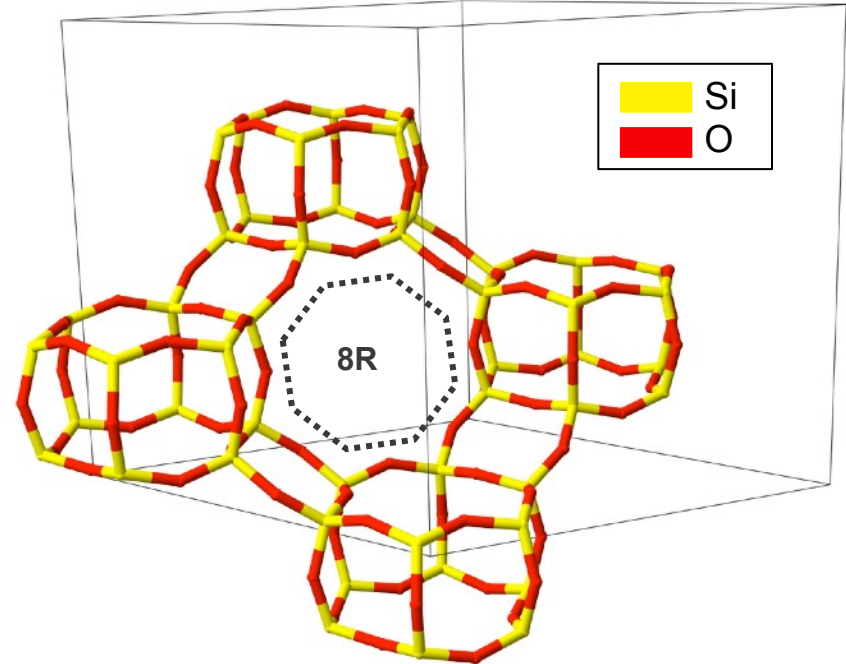
Chabazite (CHA)

- Microporous, crystalline aluminosilicate solids
- Petrochemical processing
 - Cracking, isomerisation and alkylation
- Increasing concern for the environment has motivated development of sustainable and environmentally benign alternatives to traditional petrochemical methods
- The use of traditional zeolite catalysts in atypical processes
 - Pollution control
 - Hydrocarbon production



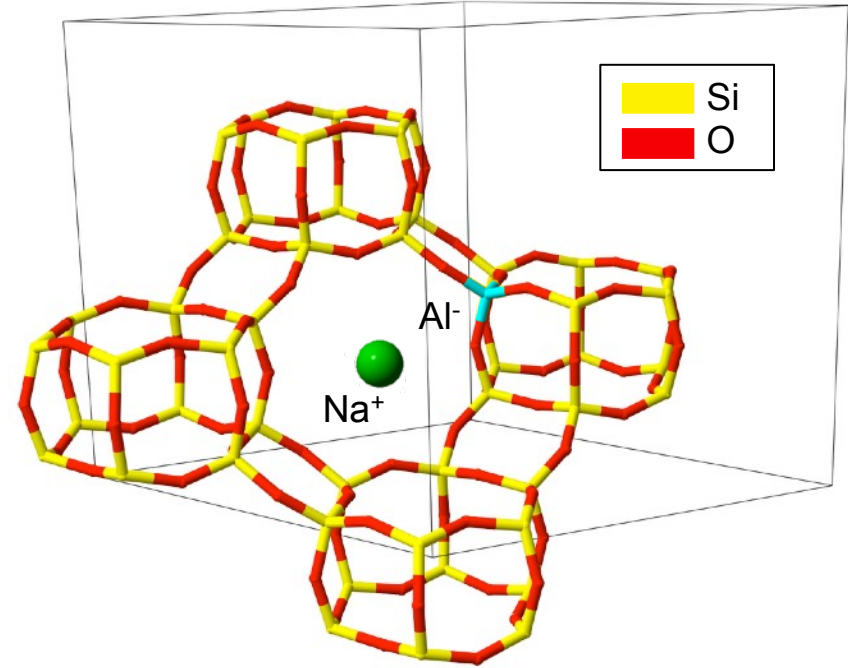
SSZ-13 (CHA)

- Microporous, crystalline aluminosilicate solids
- Petrochemical processing
 - Cracking, isomerisation and alkylation
- Increasing concern for the environment has motivated development of sustainable and environmentally benign alternatives to traditional petrochemical methods
- The use of traditional zeolite catalysts in atypical processes
 - Pollution control
 - Hydrocarbon production



SSZ-13 (CHA)

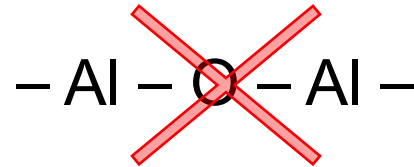
- Substituting tetravalent silica with trivalent alumina introduces a negative charge to the zeolite framework
- Charge-balancing counter cations (K^+ , Na^+ , Cu^{2+} , H^+)
- Generally accepted that Al and associated cations play a crucial role in catalysis, particularly protonated zeolites, in which a Brønsted acidic site is formed.
- Before we can begin to investigate catalytic mechanisms, and design new zeolite catalysts, we first need a full understanding of Al's framework location.



SSZ-13 (CHA)

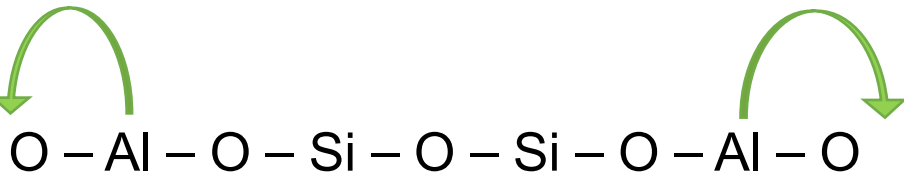
Löwenstein's Rule – 1954

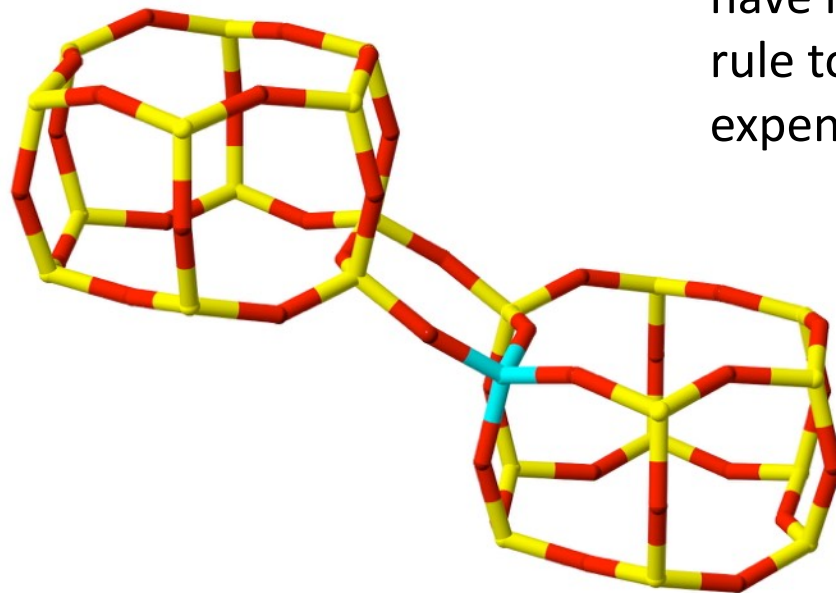
“ There is a disinclination for T-O-T linkages of adjacent tetrahedral units to possess more than one aluminium atom, forbidding the formation of Al-O-Al bonds within the zeolite framework. ”



Dempsey's Rule – 1969

“ On the basis of electrostatic arguments, framework Aluminium ions assume the furthest distance from one another. ”

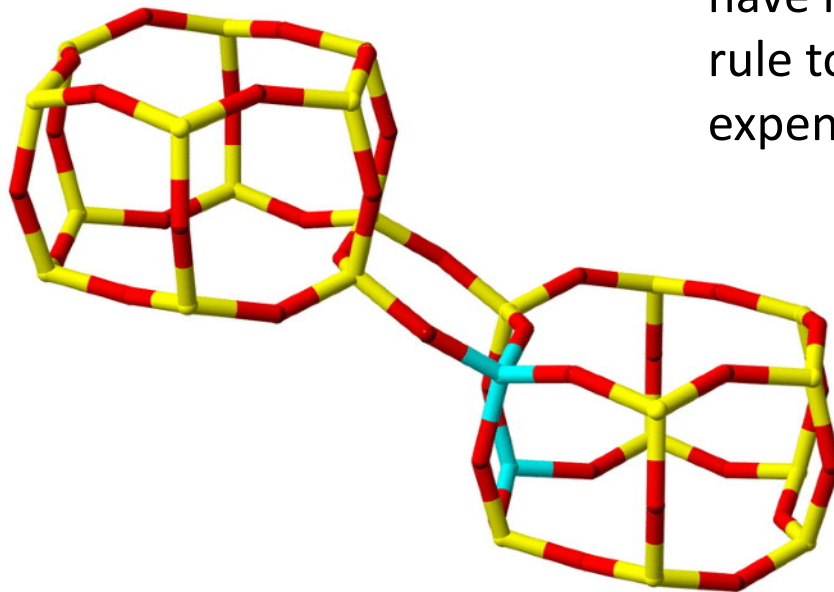




Previous investigations have invoked Lowenstein's rule to reduce computational expenditure.

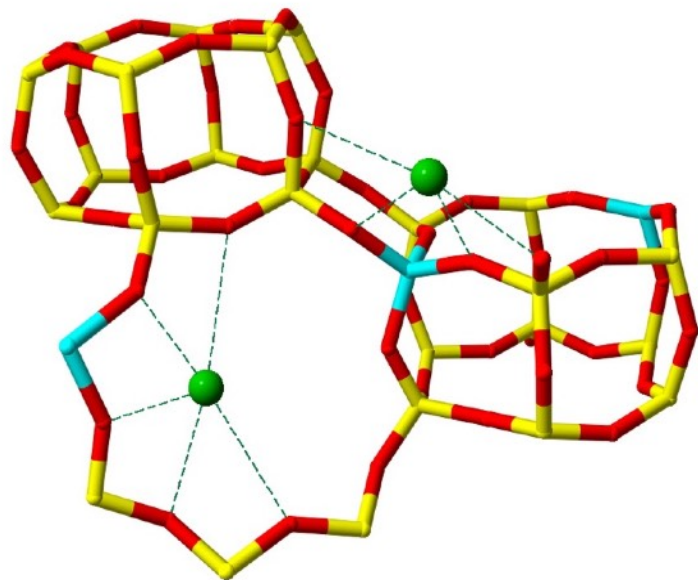
2 Al per unit cell (Si/Al = 17)

Previous investigations have invoked Lowenstein's rule to reduce computational expenditure.



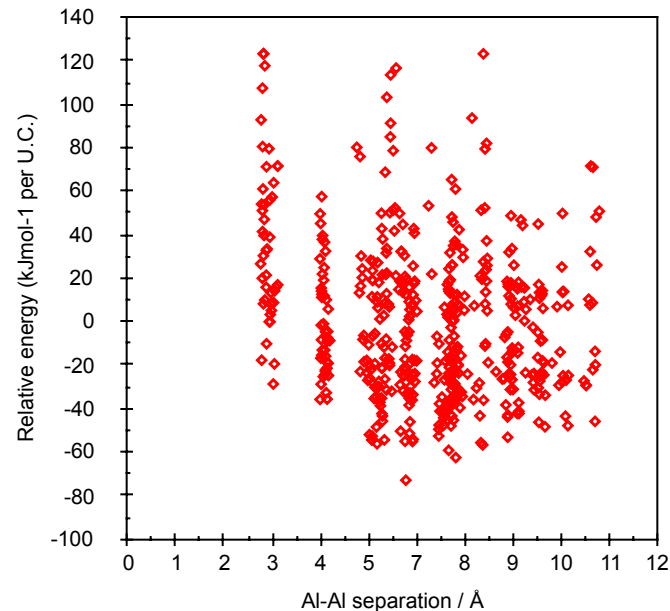
2 Al per unit cell (Si/Al = 17)

'Löwensteinian' global minimum structure



2 Al per unit cell (Si/Al = 17)

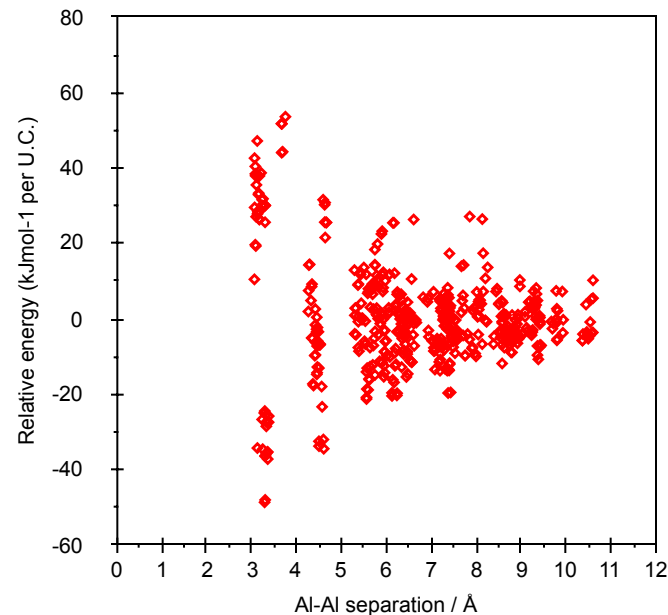
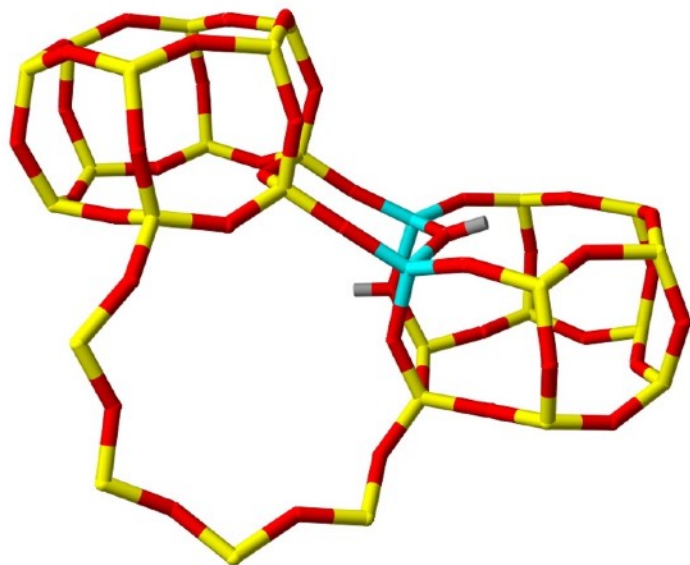
CP2K, GGA – PBE functional, TZV2P basis



$$\Delta E(N_{L_{\text{global minimum}}} - L_{\text{global minimum}}) = +44 \text{ kJ mol}^{-1} \text{ per U.C.}$$

'non-Löwensteinian' global minimum structure

CP2K, GGA – PBE functional, TZV2P basis



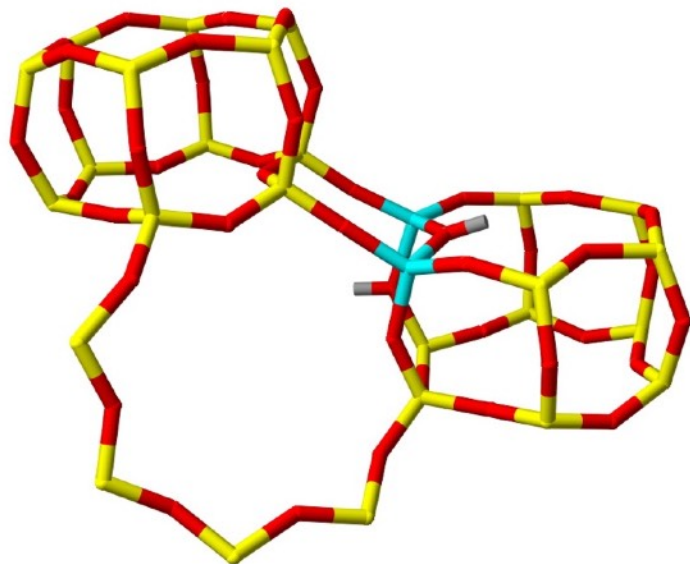
2 Al per unit cell (Si/Al = 17)

$$\Delta E(NL_{\text{global minimum}} - L_{\text{global minimum}}) = -14 \text{ kJ mol}^{-1} \text{ per U.C.}$$

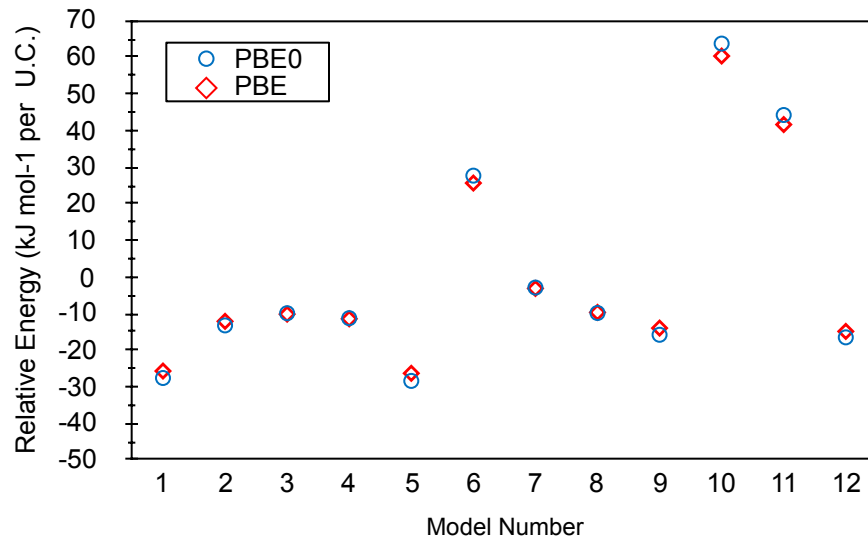
DFT data H-SSZ-13 Si/Al = 17

'non-Löwensteinian' global minimum structure

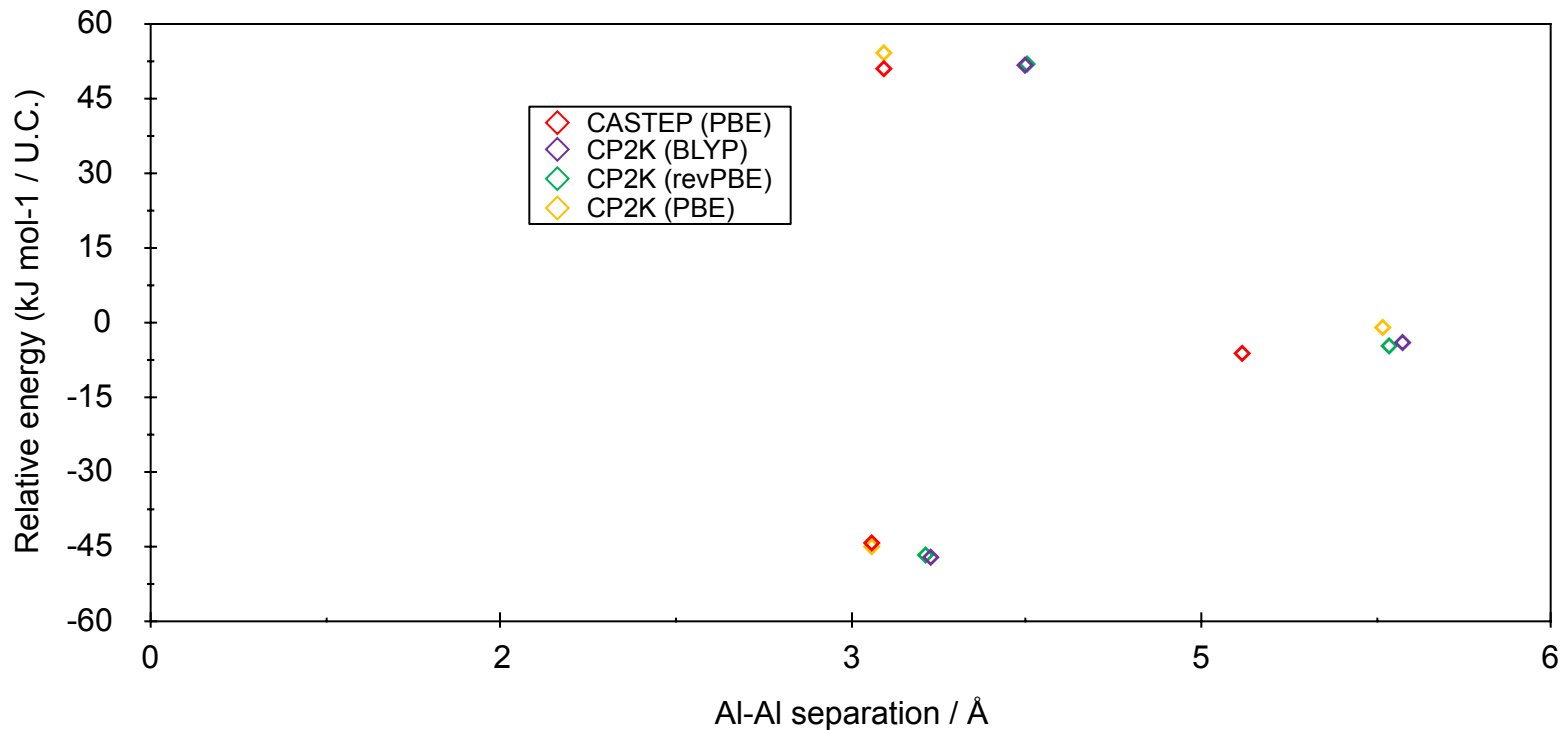
CP2K, GGA – PBE functional, TZV2P basis



2 Al per unit cell (Si/Al = 17)



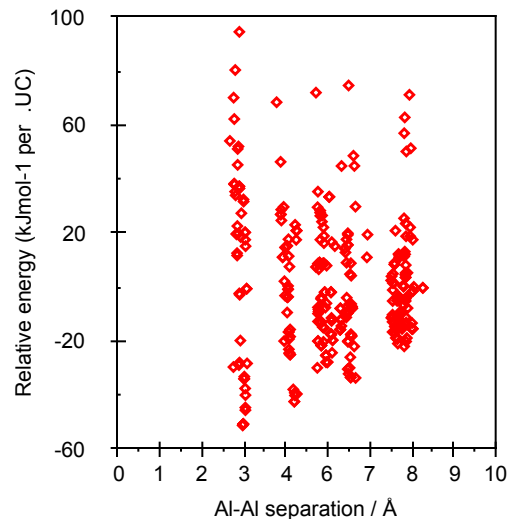
$$\Delta E(NL_{\text{global minimum}} - L_{\text{global minimum}}) = -14 \text{ kJ mol}^{-1} \text{ per U.C.}$$



Other zeolites

$$\Delta E(NL_{\text{global minimum}} - L_{\text{global minimum}})$$

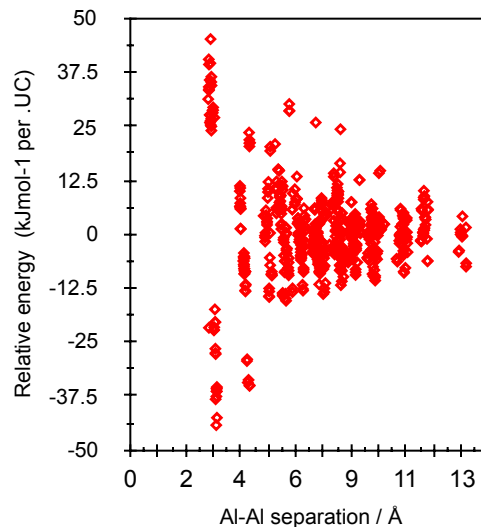
-8.3 kJ mol⁻¹ per U.C.



LTA

Density = 14.2 Tnm⁻¹
(CHA = 15.1 Tnm⁻¹)

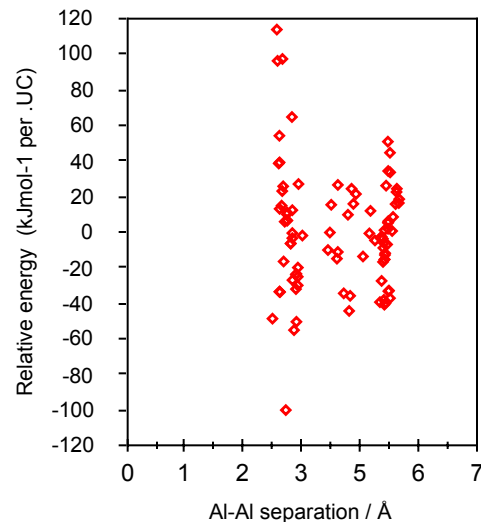
-9.2 kJ mol⁻¹ per U.C.



RHO

14.5 Tnm⁻¹

-55.7 kJ mol⁻¹ per U.C.

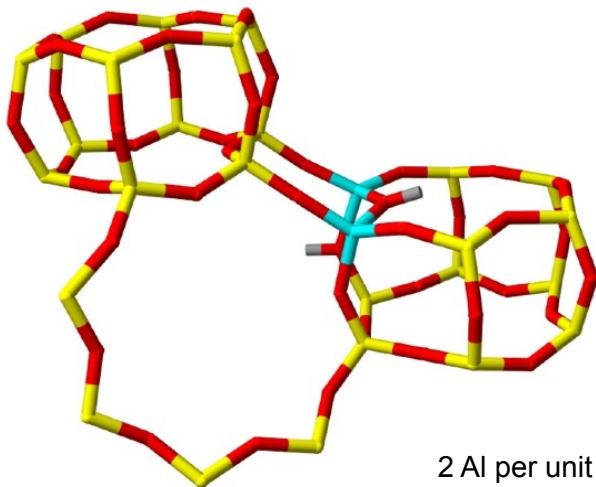


ABW

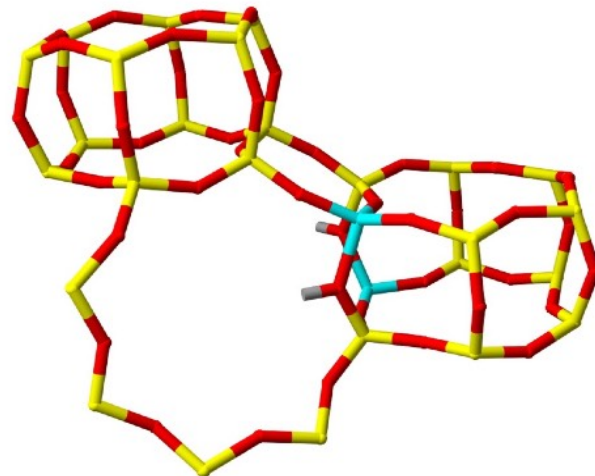
16.1 Tnm⁻¹

But why?

'non-Löwensteinian' global minimum structure



'Löwensteinian' global minimum structure



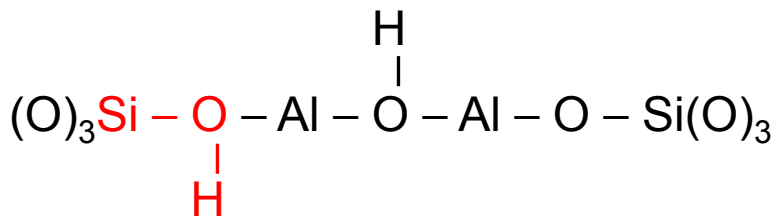
2 Al per unit cell (Si/Al = 17) H-S

+14 kJ mol⁻¹

But why?

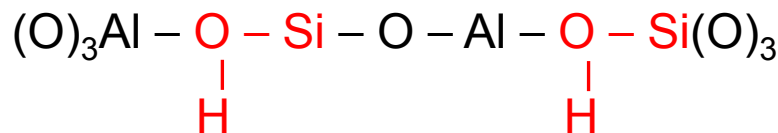
'non-Löwensteinian' global minimum structure

3 Al-O(H) linkages
1 Si-O(H) linkage



'Löwensteinian' global minimum structure

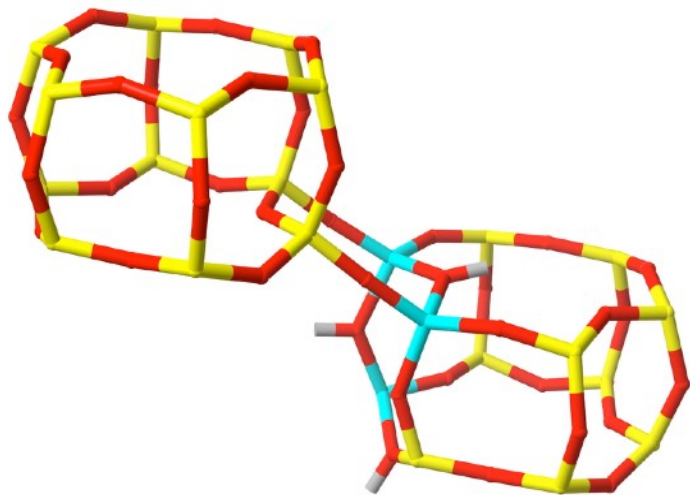
2 Al-O(H) linkages
2 Si-O(H) linkages



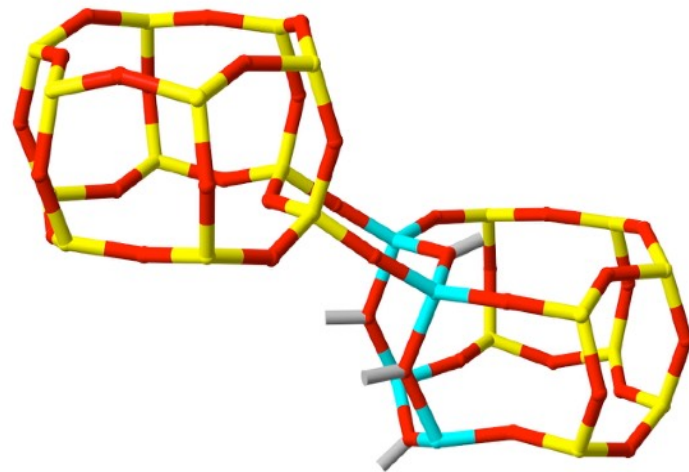
kT approx 5kJ/mol

Free energy difference is comparable to internal energy difference

Na-SSZ-13 $\Delta E(\text{NL}_{\text{global minimum}} - \text{L}_{\text{global minimum}}) = +44 \text{ kJ mol}^{-1} \text{ per U.C.}$



3 Al per unit cell (Si/Al = 11)



4 Al per unit cell (Si/Al = 8)

- Potentially invaluable for understanding existing zeolite catalytic mechanisms and Brønsted acidity, to the development of new zeolite catalysts, and the synthesis of hierarchical materials.

But....

- How can we make these structures?

Reverse dealumination

- What signatures could be used to unambiguously identify these -Al-O-Al-?

^{17}O SS MAS NMR

- Evidence for non-Löwensteinian ordering in protonated zeolite frameworks
- Preference for the formation of discrete aluminium clusters in low silica frameworks.
- Not the case for sodium-containing zeolites, where the global minimum structures are Löwensteinian ordered frameworks.
- Demonstrates the the influence of counter-cation identity on framework aluminium location.
- We hope this work stimulates experimental investigation into the direct or post-synthesis of non-Löwensteinian ordered zeolites and further characterisation of existing materials

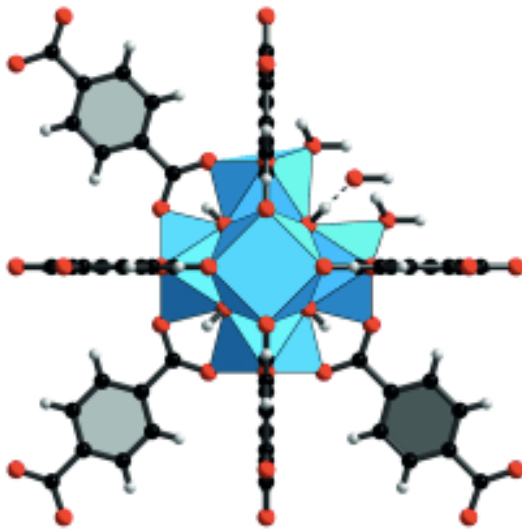
Metal-Organic Frameworks

International Edition: DOI: 10.1002/anie.201505461

German Edition: DOI: 10.1002/ange.201505461

Definitive Molecular Level Characterization of Defects in UiO-66 Crystals

*Christopher A. Trickett, Kevin J. Gagnon, Seungkyu Lee, Felipe Gándara, Hans-Beat Bürgi, and Omar M. Yaghi**



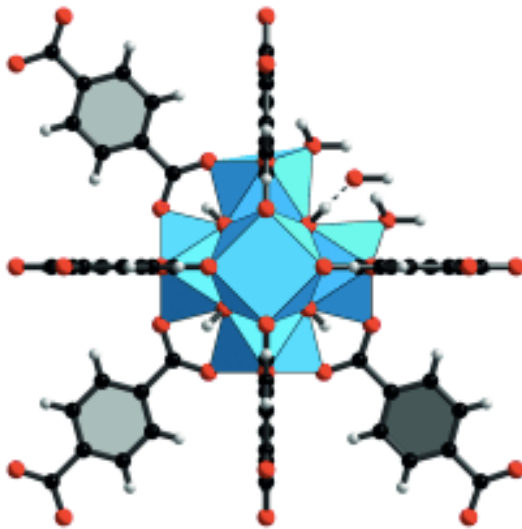
Metal-Organic Frameworks

International Edition: DOI: 10.1002/anie.201505461

German Edition: DOI: 10.1002/ange.201505461

Definitive Molecular Level Characterization of Defects in UiO-66 Crystals

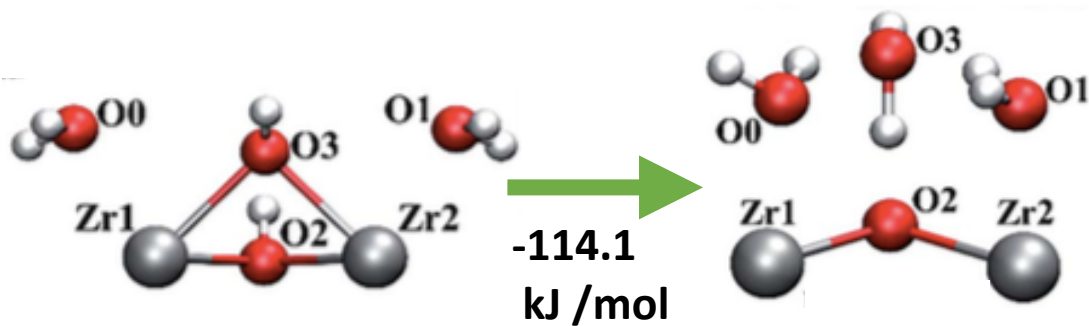
*Christopher A. Trickett, Kevin J. Gagnon, Seungkyu Lee, Felipe Gándara, Hans-Beat Bürgi, and Omar M. Yaghi**



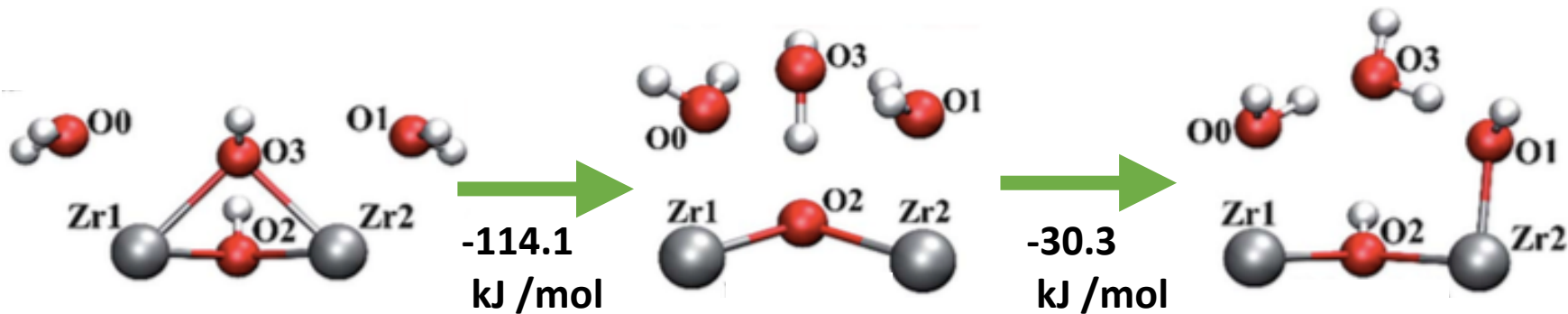
True defect structure?



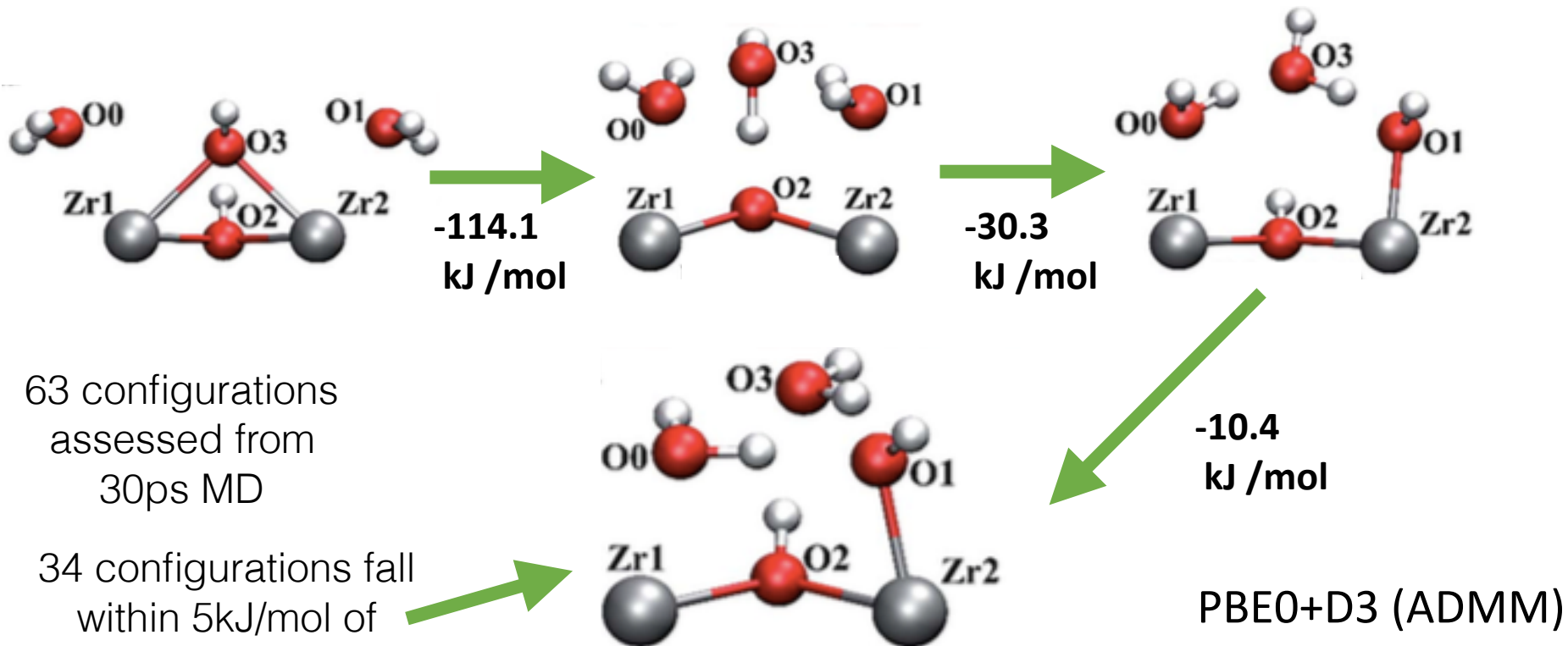
Proton *abstraction* favourable



Proton *migration* favourable

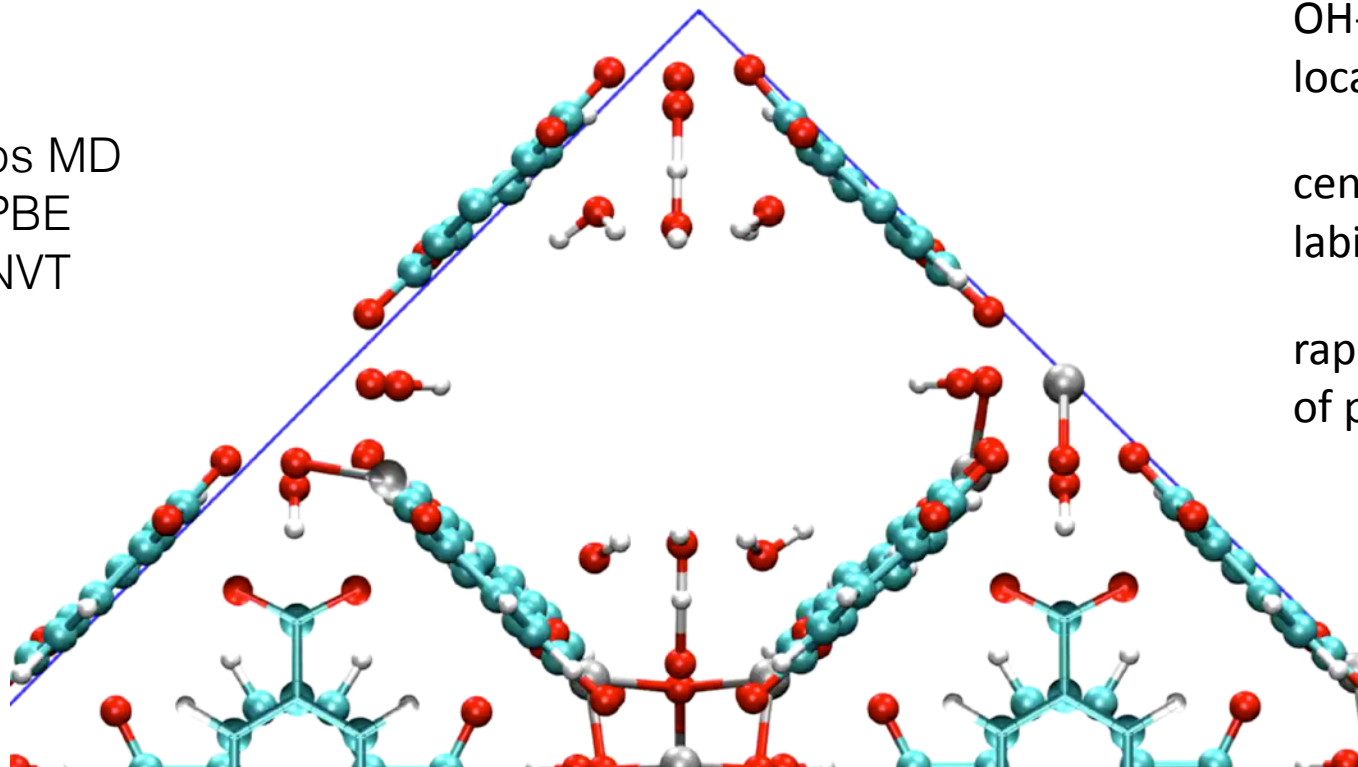


Definitive defect structure?



Defect structure is *fluxional*

30ps MD
PBE
NVT

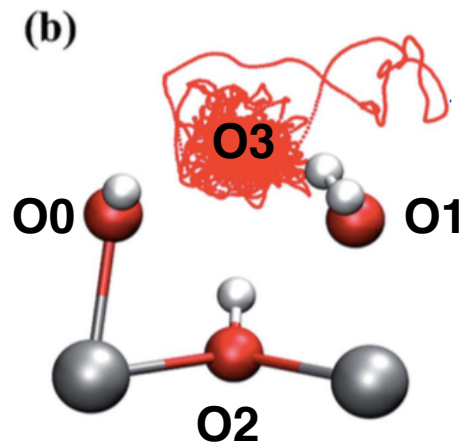
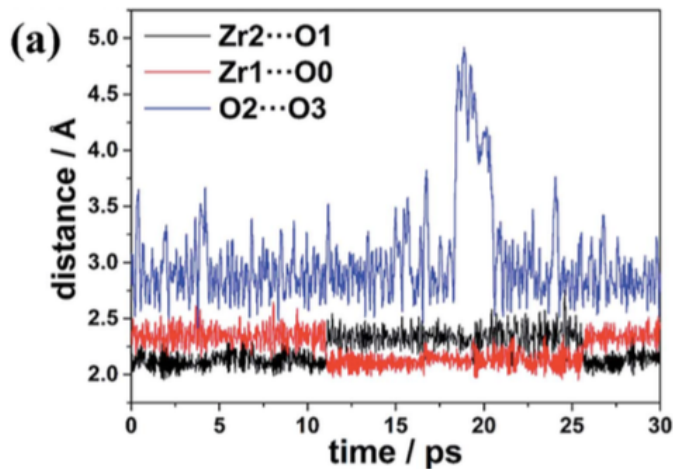


OH- proton
localised

central water is
labile

rapid interchange
of protons

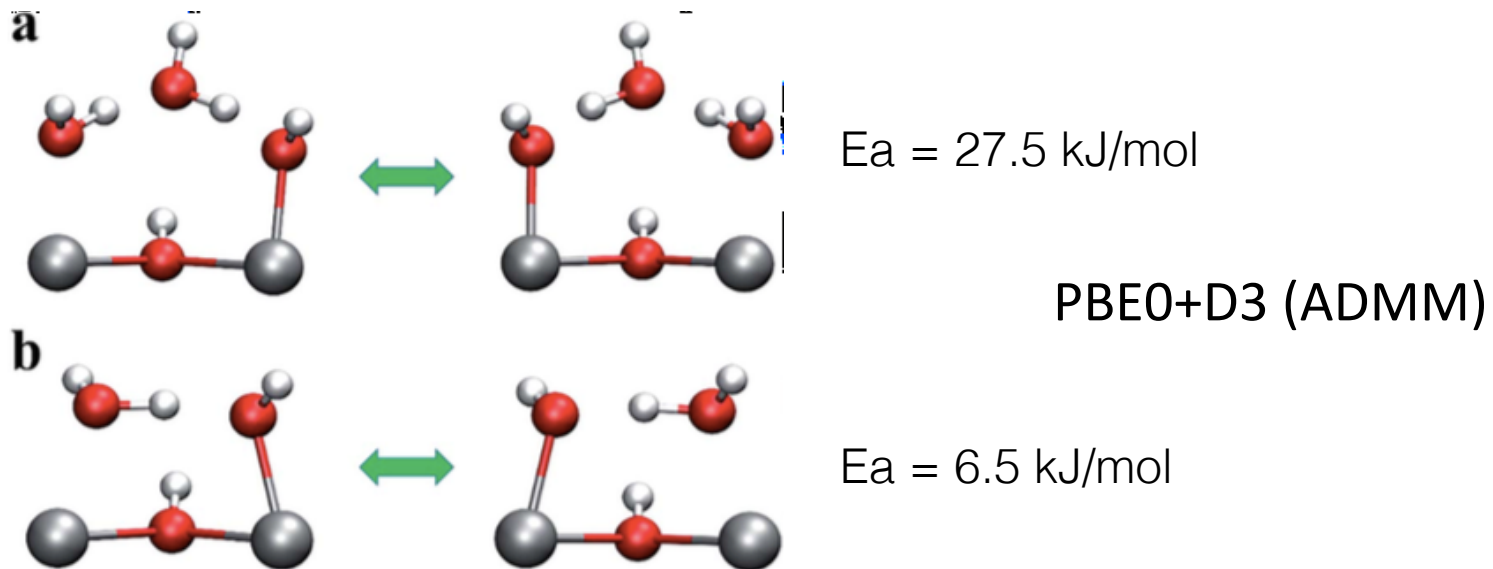
Where is the hydroxide?



Rapid exchange of protons

Static picture from XRD misses dynamic exchange

Proton migration barrier height?



Source of proton tunnelling/intrinsic proton conduction

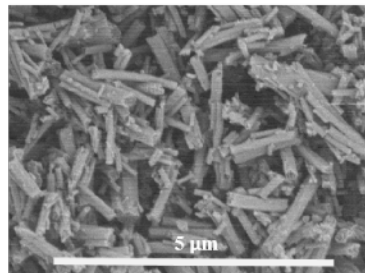
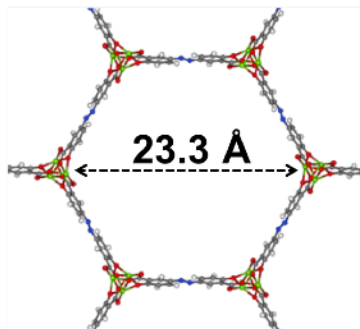
Possible frustrated Lewis acid site at high T (dehydrated)

High throughput screening of MOFs

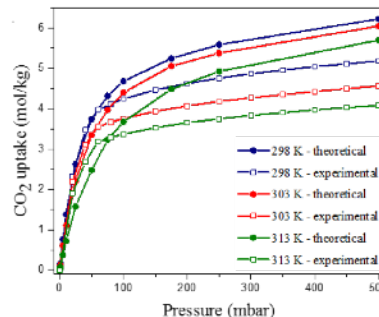
PubChem Compound Database
(~60,000,000 structures)



A total of **61**
MOF-74 Analogs



Experimental Synthesis



CO₂ Adsorption Isotherms

In collaboration with Dr Maciej Haranczyk (LBNL) and Prof Berend Smit (University of California, Berkeley and EPFL)

Table S1. Summary of partial atomic charges derived from VASP (previous work) and CP2K (this work). The naming convention of atom types can be found in the previous work.¹

Atom type	VASP/REPEAT	CP2K/REPEAT
Mg	1.56	1.66
Oa	-0.90	-0.92
Ob	-0.75	-0.76
Oc	-0.90	-0.97
Ca	0.90	0.88
Cb	-0.31	-0.32
Cc	0.46	0.48
Cd	-0.23	-0.26
H	0.19	0.21

Variance
in the
ESP is
fitted

Witman, Ling, et al., *Chem. Sci.*, **7**, 6263 (2016)

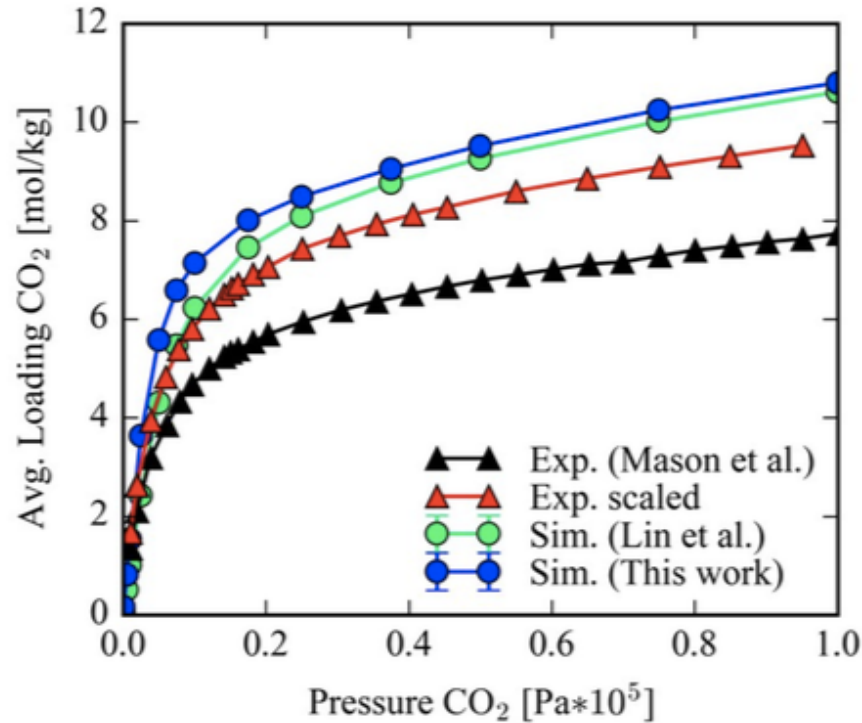
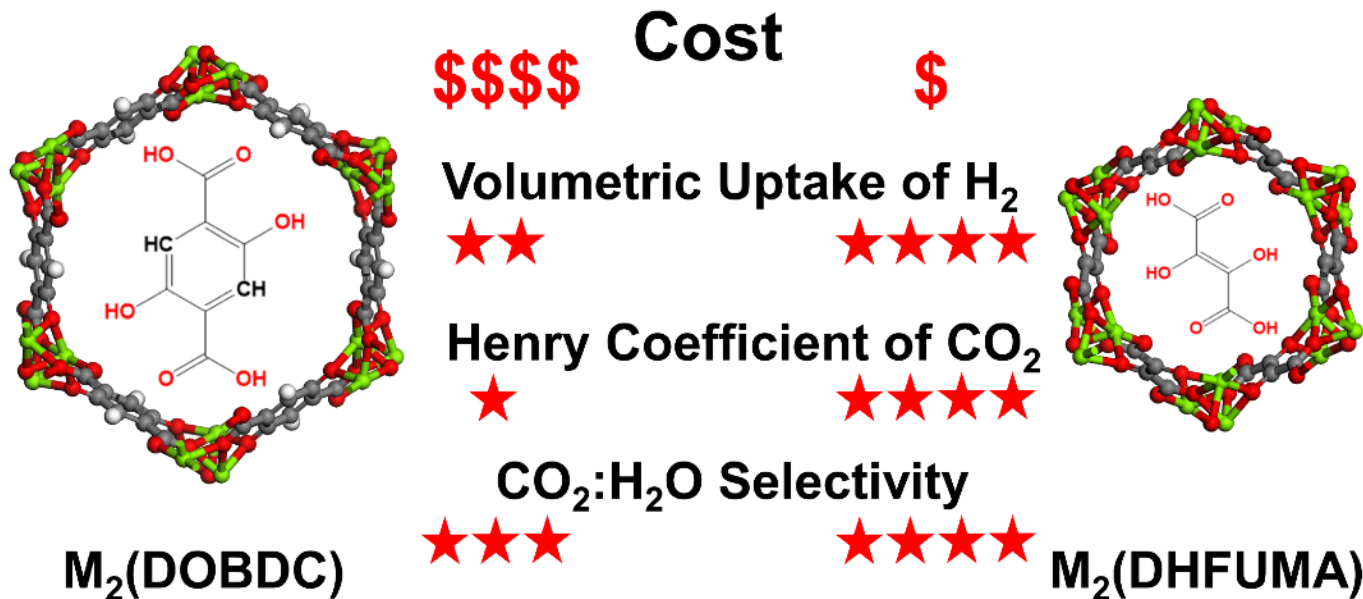


Figure S1. The CP2K relaxed structure and REPEAT derived atomic partial charges were validated by comparison of the CO₂ adsorption isotherm in the original MOF-74 structure with the previously published results of Lin et al. The experimental isotherm of Mason et al.² is scaled due to 80% accessibility of the material.

Rational design of low-cost, high-performance MOFs for hydrogen storage and carbon capture



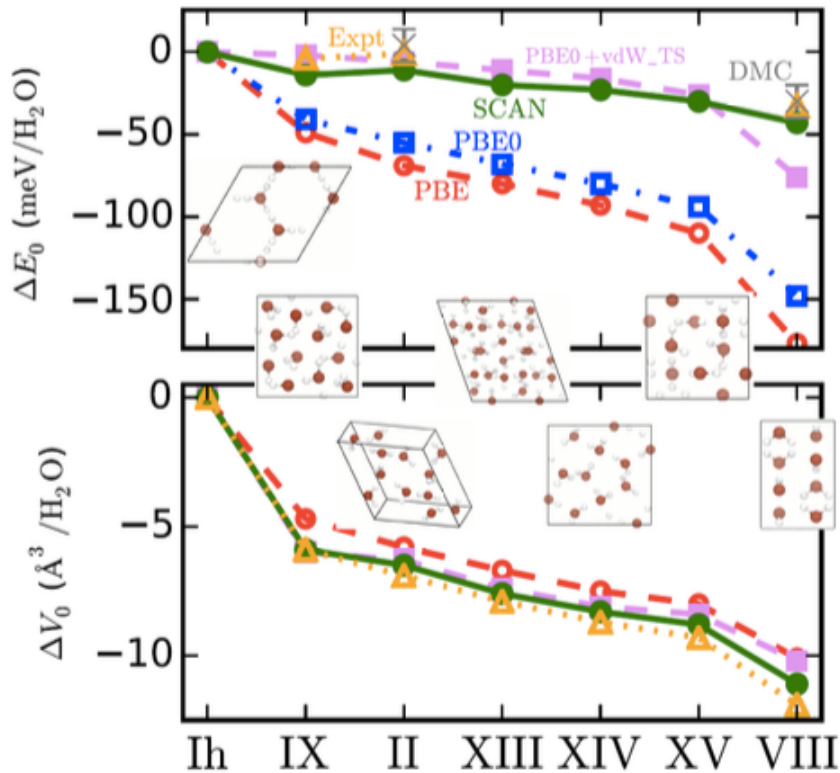
Accurate first-principles structures and energies of diversely bonded systems from an efficient density functional

Jianwei Sun^{1*}, Richard C. Remsing^{2,3}, Yubo Zhang¹, Zhaoru Sun¹, Adrienn Ruzsinszky¹, Haowei Peng¹, Zenghui Yang¹, Arpita Paul⁴, Umesh Waghmare⁴, Xifan Wu¹, Michael L. Klein^{1,2,3} and John P. Perdew^{1,2}

One atom or molecule binds to another through various types of bond, the strengths of which range from several meV to several eV. Although some computational methods can provide accurate descriptions of all bond types, those methods are not efficient enough for many studies (for example, large systems, *ab initio* molecular dynamics and high-throughput searches for functional materials). Here, we show that the recently developed non-empirical strongly constrained and appropriately normed (SCAN) meta-generalized gradient approximation (meta-GGA) within the density functional theory framework predicts accurate geometries and energies of diversely bonded molecules and materials (including covalent, metallic, ionic, hydrogen and van der Waals bonds). This represents a significant improvement at comparable efficiency over its predecessors, the GGAs that currently dominate materials computation. Often, SCAN matches or improves on the accuracy of a computationally expensive hybrid functional, at almost-GGA cost. SCAN is therefore expected to have a broad impact on chemistry and materials science.

Sun et al. Nature Chemistry, **8**, 831, 2016

The SCAN functional: the good




The SCAN functional: the good

Method	ΔE (kJ/mol/Zn)			MAD
	ZIF-1	ZIF-4	ZIF-zni	
PBE	0.27	-0.46	0.00	8.05
PBE+D3+C9	16.80	16.97	0.00	8.93
rVV10	20.76	20.42	0.00	12.63
M06L	22.04	21.20	0.00	13.66
M06L+D3	25.70	24.79	0.00	17.29
SCAN	10.11	9.44	0.00	1.82
Expt	6.88	9.03	0.00	

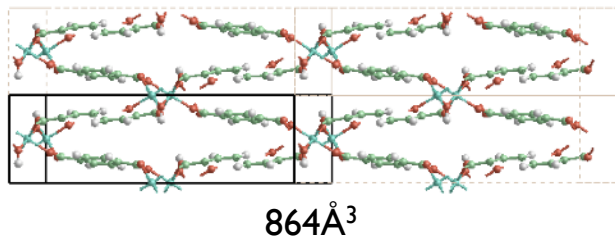
The SCAN functional: the bad

Method	ΔE (kJ/mol/Si)	ΔE (kJ/mol/Si)	ΔE (kJ/mol/Si)	
	quartz	MFI	FAU	MAD
PBE	0	0.4	2.0	9.67
PBE+D3	0	9.4	13.9	<u>0.73</u>
PBE+D3+C9	0	8.5	12.6	<u>0.64</u>
PBEsol+D3	0	7.1	10.9	<u>1.91</u>
HSE06+D3+C9	0	6.6	11.1	<u>2.05</u>
vdW-DF	0	9.8	14.8	<u>1.37</u>
vdW-DF2	0	8.9	14.1	<u>0.62</u>
optB88	0	12.6	17.9	4.35
optPBE	0	12.0	17.3	3.73
rVV10	0	10.8	15.6	<u>2.31</u>
C09X-vdW	0	13.5	18.1	4.90
SCAN (expt)	0	6.7	8.7	3.19
Expt	0	8.2	13.6	

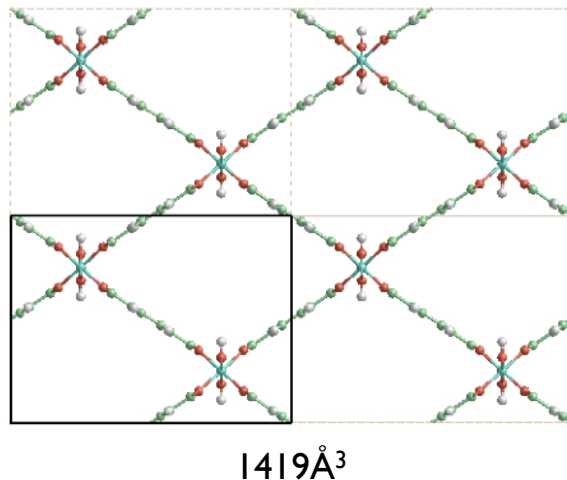
The SCAN functional: the bad

Method	ΔE (kJ/mol/Si)	ΔE (kJ/mol/Si)	ΔE (kJ/mol/Si)		
	quartz	MFI	FAU	MAD	
PBE	0	0.4	2.0	9.67	
PBE+D3	0	9.4		<u>0.73</u>	
PBE+D3+C9	0	8.5		<u>0.64</u>	
PBEsol+D3	0	7.1		<u>1.91</u>	
HSE06+D3+C9	0	6.6		<u>2.05</u>	
vdW-DF	0	9.8		<u>1.37</u>	
vdW-DF2	0	8.9		<u>0.62</u>	
optB88	0	12.6		4.35	
optPBE	0	12.0		3.73	
rVV10	0	10.8		<u>2.31</u>	
C09X-vdW	0	13.5		4.90	
SCAN (expt)	0	6.7		8.7	3.19
Expt	0	8.2		13.6	

Al-MIL-53 (Ferey et al.)



325-375K
⇌
125-150K



- In the presence of a guest (e.g. $p\text{CO}_2$), the cell volume \sim doubles
- In 2008, Brown et al., *JACS*, showed cell hysteresis in the absence of a guest.
- DFT+D and vdWDF approaches showed the dense phase is stabilised by dispersion. (\sim 8-14 kJ / mol per Al) (Exp. 7.5 kJ / mol / Al - calorimetry)
- Vibrational entropy drives the expansion (low frequency modes)

Most GGA/Hybrids: good/bad

MIL-53-AI

Method	<i>np</i> -MIL-53-AI		C	beta	volume	$\Delta E^{(np-lp)}$
	A	B				
PBE	-	-	-	-	-	-
PBE+D3	20.99	6.57	6.65	65.96	837.6	-8.66
PBEsol+D3	21.03	6.28	6.61	64.93	791.4	-10.54
PBE+D3+C9	20.95	6.73	6.66	66.25	858.8	-3.85
HSE06+D3+C9	20.78	6.75	6.61	66.35	848.8	-3.1
vdW-DF	20.92	6.71	6.69	67.51	867.6	-10.88
C09x-vdW	21.05	5.95	6.6	65	749.7	-27.99
optB88	21.07	6.08	6.62	65.02	768.7	-25.82
optPBE	20.96	6.28	6.66	66.87	807.3	-21
vdW-DF2	20.8	6.46	6.73	69.32	845.1	-7.36
rVV10	20.93	6.34	6.67	67.62	818	-14.43
Expt^b	20.82	6.87	6.61	66.05	863.9	-7.5

MIL-53-AI

Fixed_expt_lattice		kJ/mol per Al center
lp_ortho_symm-np	SCAN	-4.38
lp_ortho_symm-np	M06-L	17.16
lp_ortho_symm-np	PBE+D3+C9	5.79
Fixed_PBE+D3+C9_lattice		kJ/mol per Al center
lp_ortho_symm-np	SCAN	-4.91
lp_ortho_symm-np	PBE+D3+C9	4.72

see The polymorphism of ice: five unresolved questions, Salzmann et al., PCCP, 2011

THE JOURNAL OF
PHYSICAL CHEMISTRY
Letters

Letter


pubs.acs.org/JPLC

[dx.doi.org/10.1021/jz401625w](https://doi.org/10.1021/jz401625w) | *J. Phys. Chem. Lett.* 2013, 4, 3165–3169

What Governs the Proton Ordering in Ice XV?

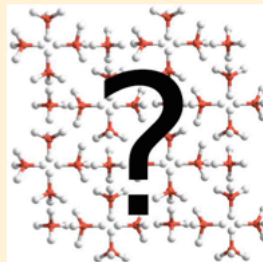
Kaushik D. Nanda and Gregory J. O. Beran*

Department of Chemistry, University of California, Riverside, California 92521, United States

 Supporting Information

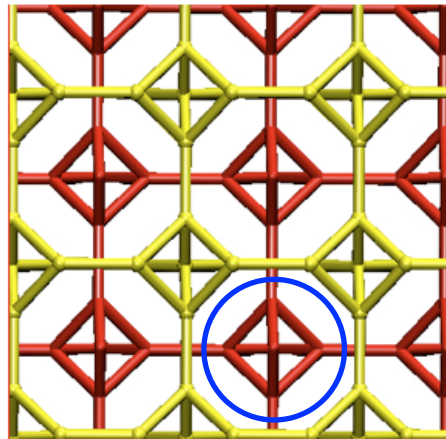
ABSTRACT: Powder neutron diffraction and Raman spectroscopy experiments for ice XV, the recently discovered proton-ordered polymorph of ice VI, suggest that the protons arrange in an antiferroelectric structure with $P\bar{1}$ symmetry, contrary to several density functional theory predictions of a ferroelectric Cc structure. Here, we find that higher-level fragment-based second-order perturbation theory (MP2) and coupled cluster theory (CCSD(T)) electronic structure calculations predict that the experimentally proposed proton ordering is indeed slightly more stable than the other possible structures. These calculations reveal a close competition between the structure with the strongest local hydrogen bonding (Cc) and the one with the most favorable "delocalized" hydrogen bond cooperativity effects ($P\bar{1}$), with the latter being preferred by ~ 0.4 kJ/mol per molecule. The results reiterate the importance of viewing ice networks as a whole instead of focusing on pairwise hydrogen-bonding interactions.

SECTION: Molecular Structure, Quantum Chemistry, and General Theory



Ice XV/VI
have the
largest
variation in
hydrogen
bond angle of
any phase.

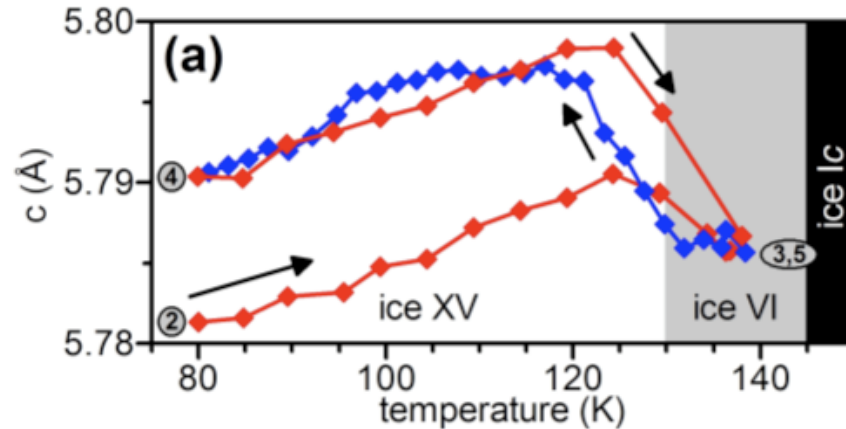
Problem solved?



VI - SG I 37

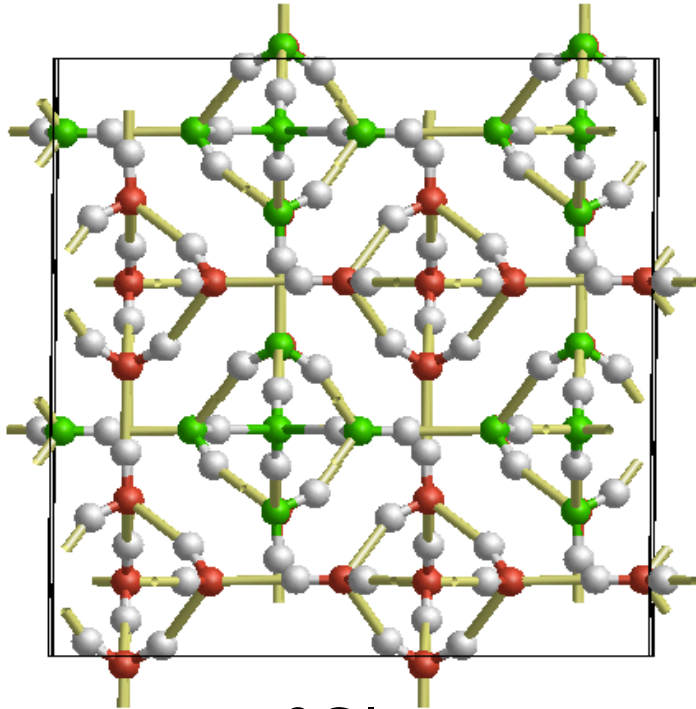
↓
XV - SG 2

Interpenetrating
lattices formed from
hexameric chains

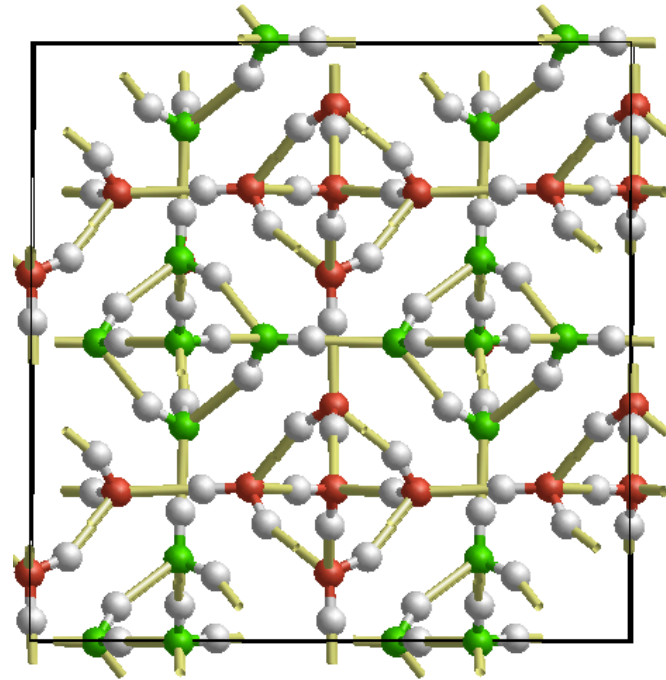


XRD data taken from Salzmann et al. PRL 2009

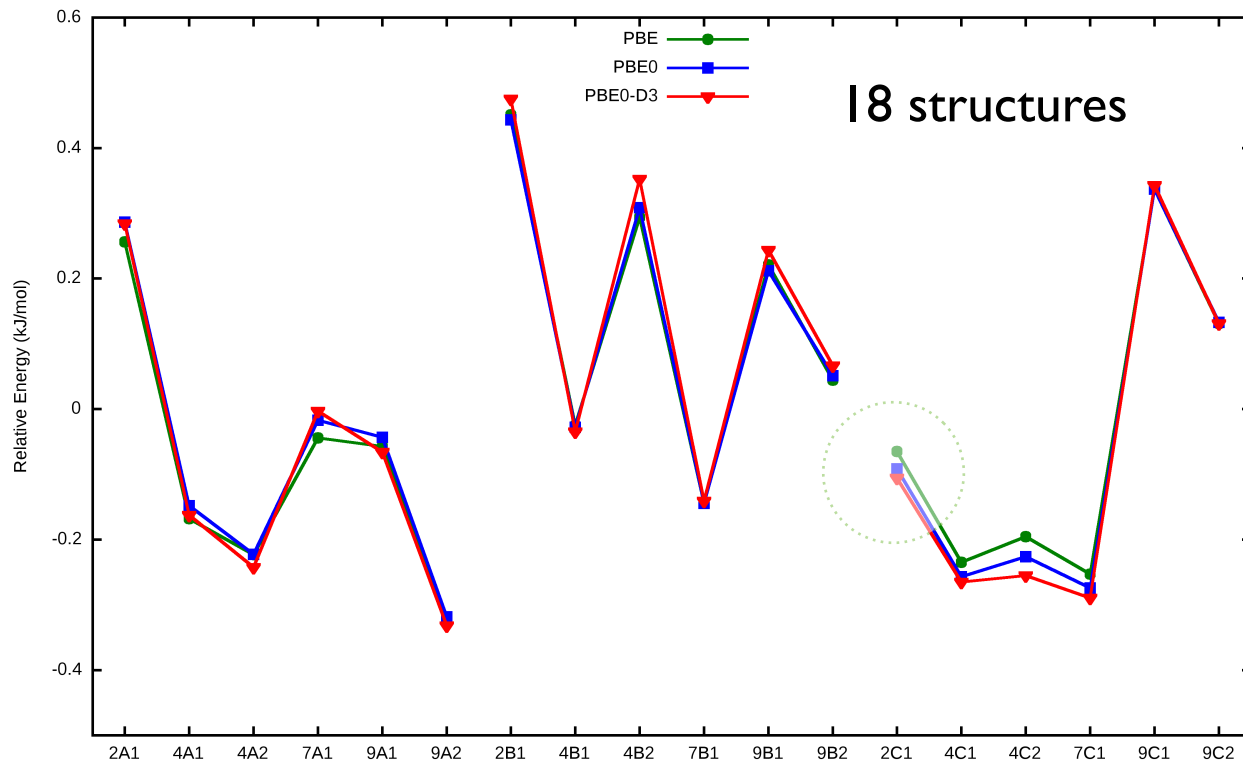
Dense structure (~ 1 GPa)



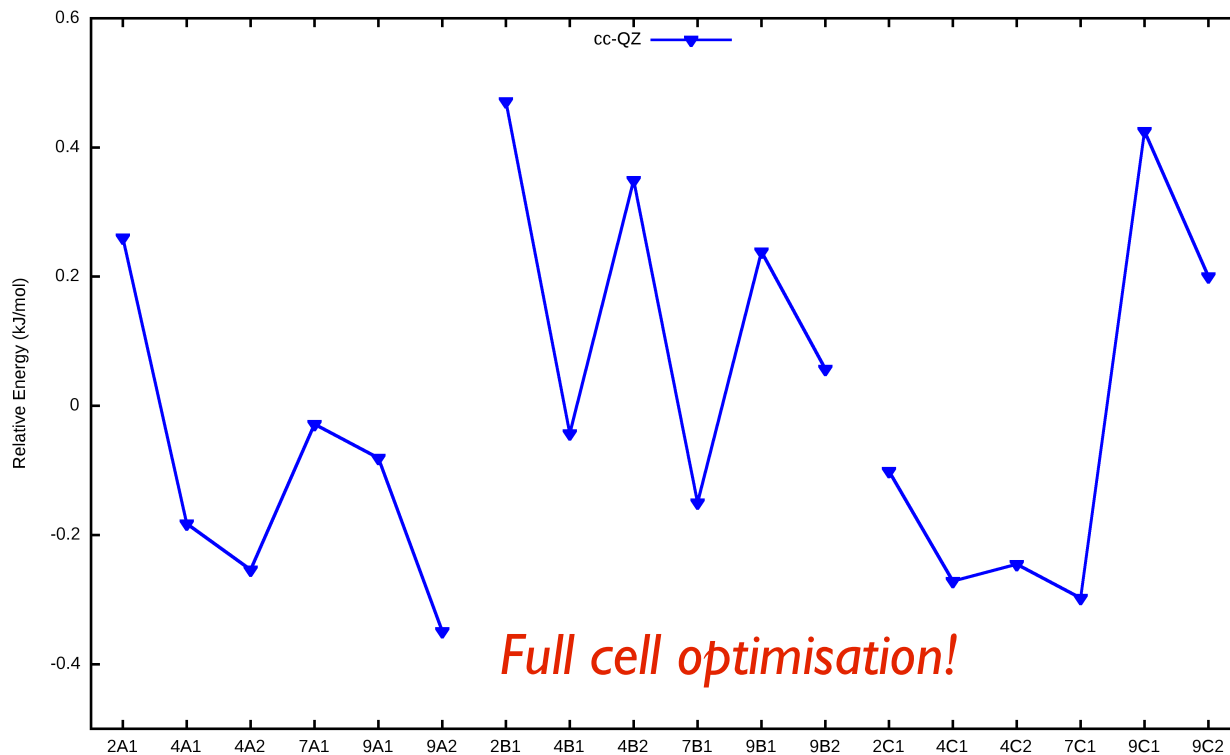
2CI



9A2



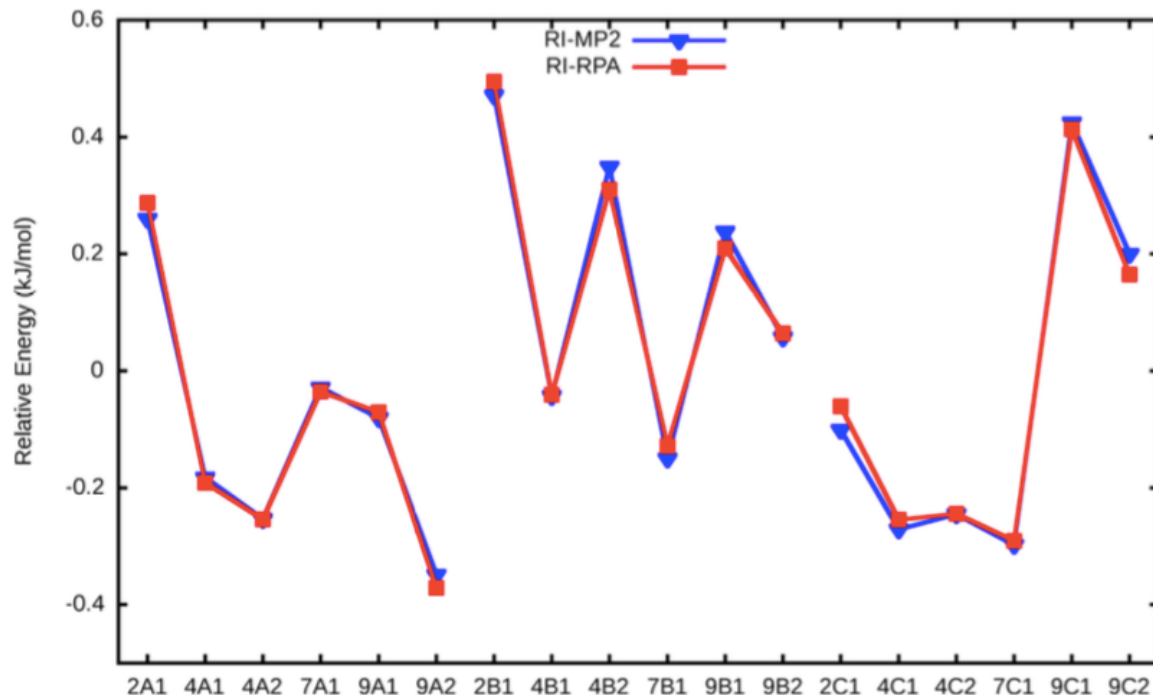
Varying HF and vdW does not change
the order of stability



Full cell optimisation!

9A2 = Cc most stable 1078s on 3840 processors (Archer)

Theory still predicts exptl (2C1) structure to be metastable

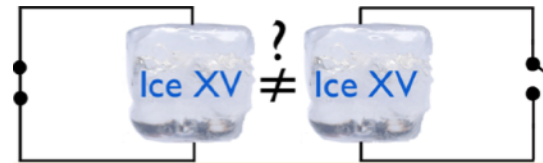
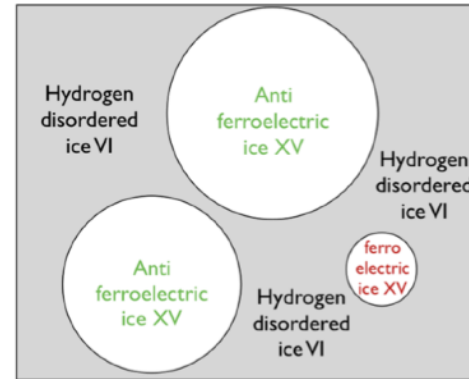
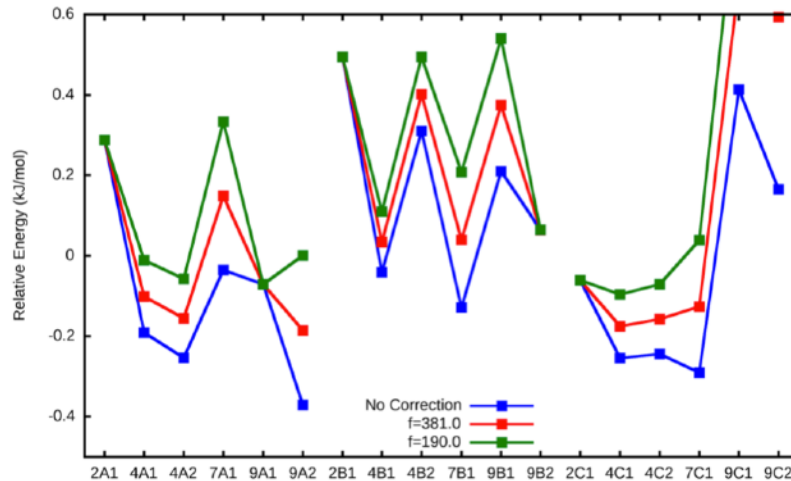


9A2 = Cc most stable 1078s on 3840 processors (Archer)

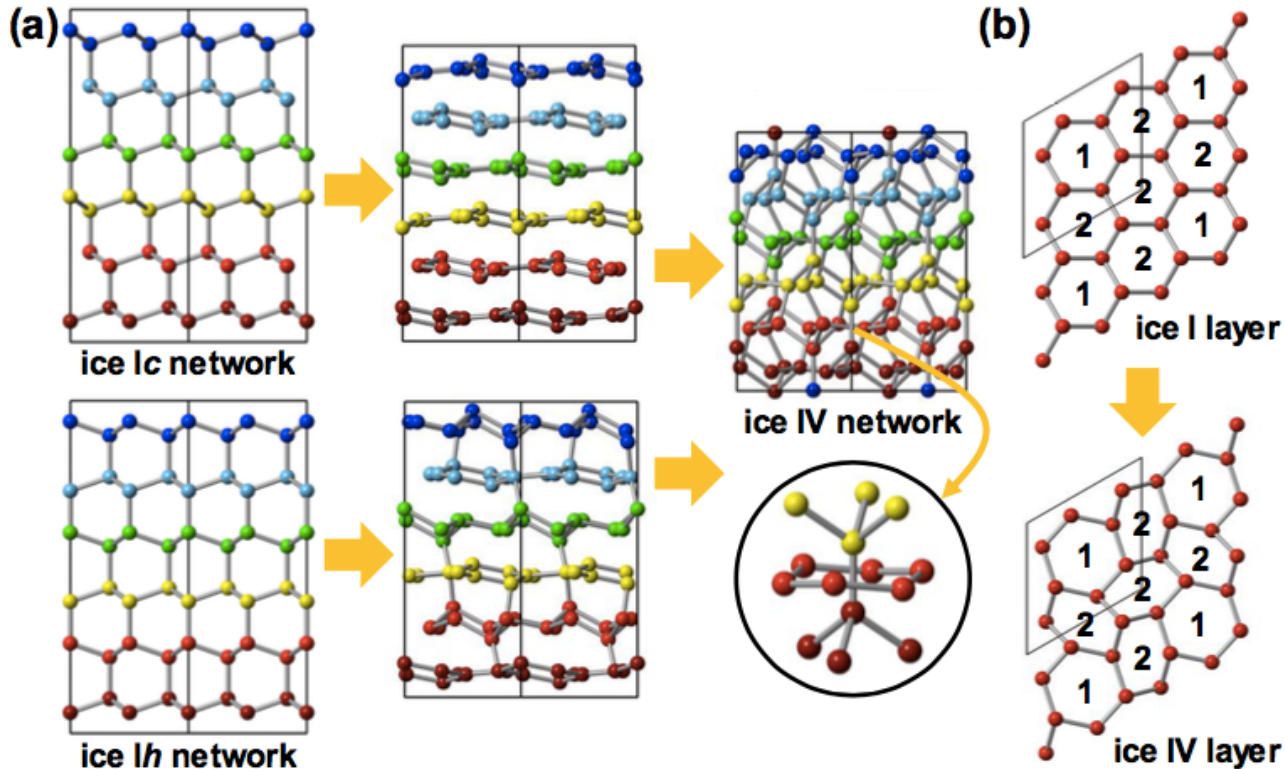
Theory still predicts exptl (2C1) structure to be metastable

Theory still predicts wrong ground state
 Experimentally, only about 70% of ice VI → XV
 Grains of ice XV in a matrix of VI

$$U_{\text{corr}} = \frac{2\pi}{Vf} M^2$$

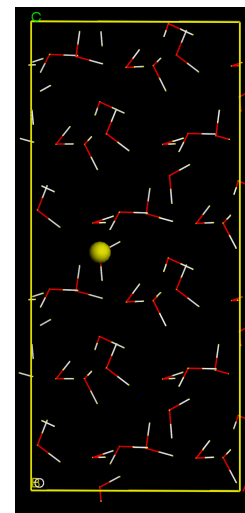
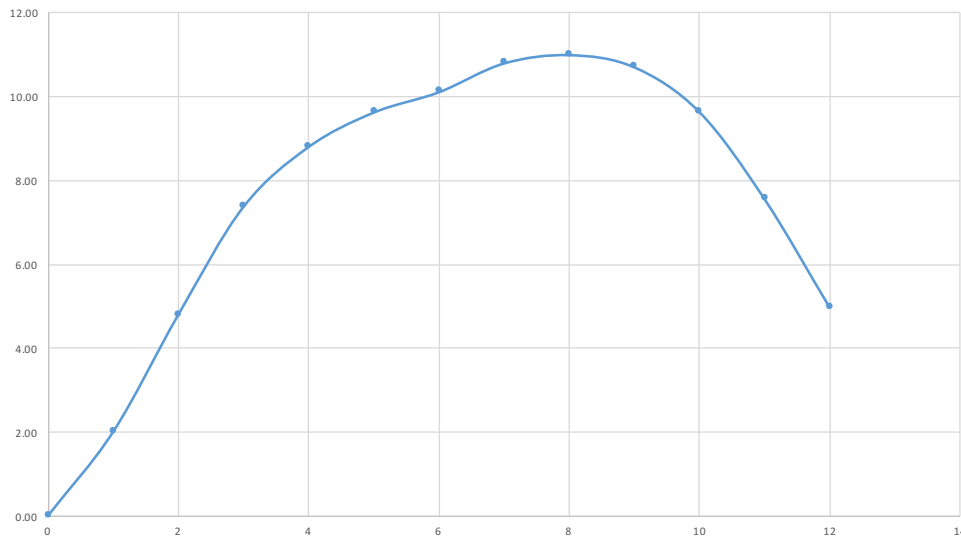
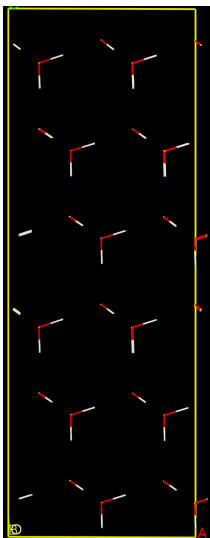


Solid state NEB - ice XIc-IV



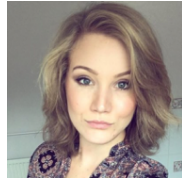
Solid state NEB - ice XIc-IV

D. Sheppard, P. Xiao, W. Chemelewski, D. D. Johnson, and G. Henkelman, A generalized solid-state nudged elastic band method, *J. Chem. Phys.* **136**, 074103 (2012).



XIc (0.93) to IV (1.27 g/cm³)

Acknowledgements



Dr. Sanliang Ling

Miss Rachel Fletcher

MOF-74

Matthew Whitman (Berkeley)

Liangheng Tong (formerly KCL)

Dr Maciej Haranczyk (LBNL)

Prof Berend Smit (University of California, Berkeley and EPFL)

Ice XV - MP2/RPA

Mauro del Ben (LBNL)

Joost VandeVondele (Formerly ETH, now ?)

Unpublished work - SS-NEB

Jacob Shephard (Edinburgh)

Christoph Salzmann (UCL)



Engineering and Physical Sciences
Research Council



THE ROYAL
SOCIETY